Sensors and Actuators B 155 (2011) 159–164

Contents lists available at ScienceDirect

Sensors and Actuators B: Chemical

journal homepage: www.elsevier.com/locate/snb

Effect of surface defects on biosensing properties of TiO_2 nanotube arrays

Peng Xiao [a,c,*], Yunhuai Zhang [b,c], Guozhong Cao [c,**]

[a] College of Physics, Chongqing University, Chongqing 400044, PR China
[b] College of Chemical Engineering, Chongqing University, Chongqing 400044, PR China
[c] Department of Materials Science & Engineering, University of Washington, Seattle, WA 98195, USA

ARTICLE INFO

Article history:
Received 22 August 2010
Received in revised form
18 November 2010
Accepted 22 November 2010
Available online 27 November 2010

Keywords:
TiO_2 nanotubes
Surface defects concentration
Annealing
Enzyme
Hydrogen peroxide

ABSTRACT

In this paper, highly ordered titania nanotube (TNT) arrays fabricated by anodization were annealed at different temperatures in CO to create different concentrations of surface defects. The samples were characterized by SEM, XRD and XPS. The results showed different concentrations of Ti^{3+} defects were doped in TNT arrays successfully. Furthermore, after co-immobilized with horseradish peroxidase (HRP) and thionine chloride (Th), TNT arrays was employed as a biosensor to detect hydrogen peroxide (H_2O_2) using an amperometric method. Cyclic voltammetry results and UV–Vis absorption spectra presented that with an increase of Ti^{3+} defects concentration, the electron transfer rate and enzyme adsorption amount of TNT arrays were improved largely, which could be ascribed to the creation of hydroxyl groups on TNT surface due to dissociative adsorption of water by Ti^{3+} defects. Annealing in CO at 500 °C appeared to be the most favorable condition to achieve desirable nanotube array structure and surface defects density (0.27%), thus the TNT arrays showed the largest adsorption amount of enzyme (9.16 μg/cm^2), faster electron transfer rate (1.34×10^{-3} cm/s) and the best response sensitivity (88.5 μA/mM l^{-1}).

1. Introduction

Titanium dioxide (TiO_2) is frequently used as matrix to immobilize proteins and enzymes for biomaterial and biosensor applications due to its chemical inertness, rigidity, and thermal stability [1–3]. Compared with other morphologies of TiO_2 nanostructure, highly ordered TiO_2 nanotubes (TNT) fabricated by anodization have advantages when used as biosensors: in particular, a high surface area, favorable transport pathways and very good adhesion to the substrate. It is therefore one of favorable choice as supporting matrices for proteins and biomolecules [4–7].

To improve the sensitivity of TNT-based biosensor, the following aspects have to be considered: (i) Protein or cell adsorption behavior and (ii) electron transfer rate of TNT arrays. This two aspects depend strongly on the topography, crystalline status [8,9], surface functionalization [10] and surface defects [11] of TNT arrays. Surface defects have been recognized extensively in the literatures as point defects that exist as oxygen vacancy sites in conjunction with the conversion of Ti^{4+} to Ti^{3+} located within the bridging oxygen rows of the $TiO_2(1\,1\,0)-(1\times1)$ surface. Ti^{3+} defects generation can be obtained by Ar^+ bombardment, electron beam exposure [12], thermal annealing titania at high temperatures in inert or reducing gas and low energy ultraviolet photons illumination [13,14]. Thermal annealing produces fewer defects, all Ti^{3+} type, with very little structural damage to the surface. The creation of Ti^{3+} defects has a profound effect on the electronic properties of electrode surface. We studied the electrochemical property, conductivity and photocurrent response of TiO_2 nanotubes arrays annealed in CO, N_2 and O_2 respectively, the electron transfer rate constant (k) were enhanced to be 1.34×10^{-3} cm/s for CO-annealed nanotubes due to the existing of Ti^{3+} defects. This result can be matched with that of carbon nanotube electrode (7.53×10^{-4} cm/s) and boron-doped diamond electrode (1.06×10^{-5} cm/s) [15].

Moreover, it has been shown by authors that Ti^{3+} defects were active adsorption sites for enzyme or protein, and that interesting chemistry may occur at these sites. In our previous study, we found that the enzyme adsorption amount of CO-annealed TNT was almost 3 times higher than that adsorbed on O_2-annealed TNT due to the creation of Ti^{3+} defects, which led to approximately an order of magnitude improvement of response current [16].

Because Ti^{3+} defects' responsibility for adsorption of enzyme and improvement of the electron transfer rate of TNT arrays, controlling their densities appears to be a promising method for enhancing the sensitivity of TNT biosensor. So far, few studies have focused on the effect of surface defects densities on the structure and sensitivity of TiO_2 nanotube biosensor. Therefore, in the present article, the influence of CO annealing temperature con-

* Corresponding author at: College of Physics, Chongqing University, Chongqing 400044, PR China.
** Corresponding author. Tel.: +1 206 2187224; fax: +1 206 6332980.
E-mail addresses: xiaopeng@cqu.edu.cn (P. Xiao), gzcao@u.washington.edu (G. Cao).

0925-4005/$ – see front matter © 2010 Elsevier B.V. All rights reserved.
doi:10.1016/j.snb.2010.11.041

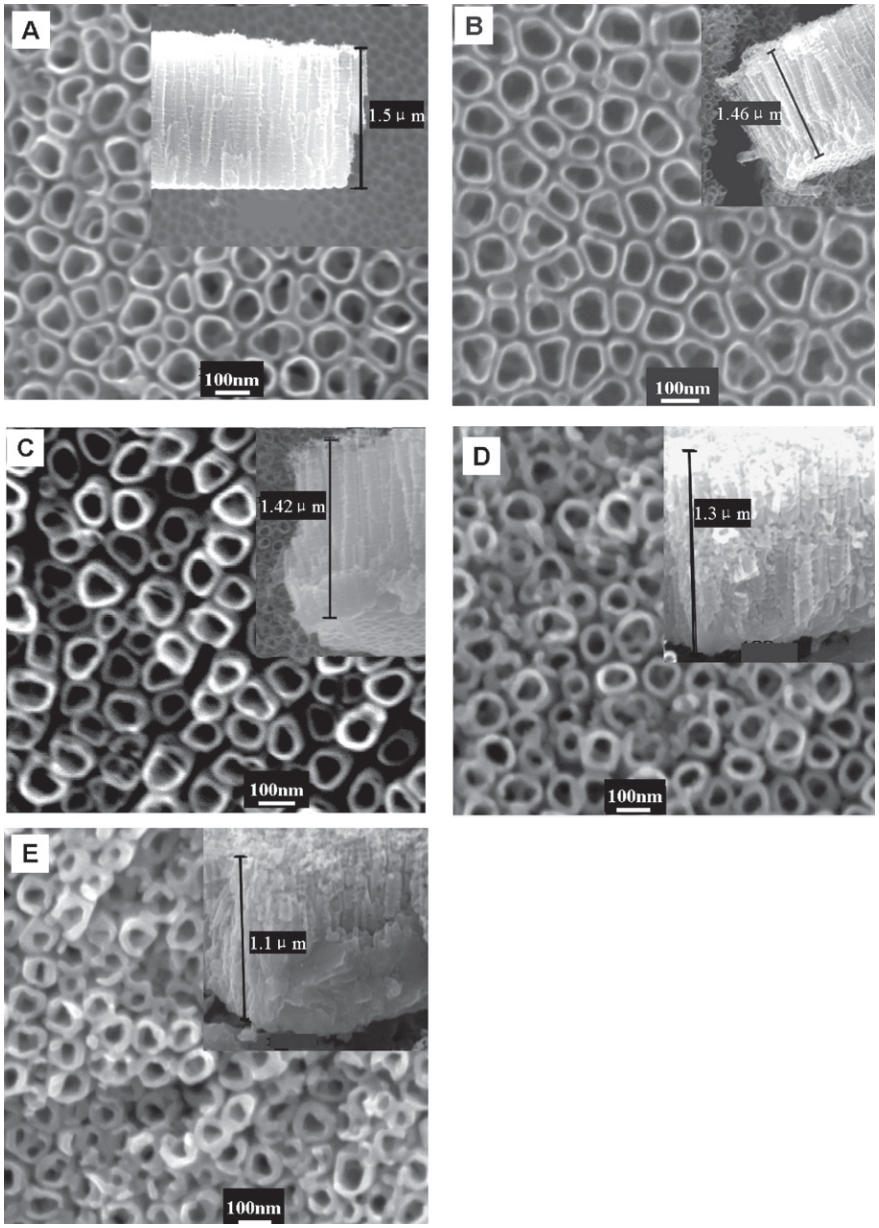

Fig. 1. SEM images of TNT arrays before (A) and after annealed in CO for 3 h at (B) 300 °C, (C) 400 °C, (D) 500 °C and (E) 600 °C.

trolling the surface defects densities are discussed with regard to X-ray photoelectron spectroscopy (XPS) analyses. The temperature range has been defined to not alter the TNT nanostructure. After co-immobilized with horseradish peroxidase (HRP) and thionin (Th), the TNT arrays were employed as a biosensor to detect hydrogen peroxide. The goal of this paper is to systematically investigate the effect of Ti^{3+} surface defects concentration on the bio-sensitivities of TNT arrays.

2. Experimental methods

Titanium foil (99% pure, 0.5 mm thick), potassium fluoride (KF, 99%), sodium hydrogen sulfate ($NaHSO_4$, 98%) were all purchased from VWR. The growth of TNT arrays by anodization has been reported widely in literatures and the growth conditions we used in this work is similar to that reported in our earlier publication [16]. The as-grown TNT arrays were annealed in CO at 300 °C, 400 °C, 500 °C and 600 °C respectively in a tube furnace with a heating rate of 5 °C/min and dwelled time of 3 h. The resultant TNT arrays are hereinafter designated as: TNT/300, TNT/400, TNT/500 and TNT/600.

The annealed TNT arrays were first sealed with epoxy resin leaving an open area of 0.5 cm^2, then immersed in 3 ml 5 mM phosphate buffer (PB) solution at pH = 7.0 containing 1.8 mg Th and 3.6 mg HRP for 24 h to produce Th/HRP modified electrodes. The resultant electrodes were stored in 5 mM PB of pH = 7.0 at 4 °C.

Surface morphologies of the TiO_2 nanotubes after annealing at different temperatures were characterized by scanning electron microscope (SEM, Philips, JEOL JSM7000). X-ray diffraction (XRD) was performed on a Philips 1820 X-ray diffractometer with Cu Ka radiation (k = 1.5418 Å). Ti^{3+} defects concentration was detected by X-ray photoelectron spectroscopy (XPS, SSL-300 system, C1s was used as reference to calibrate the peaks). UV–Vis absorption spectra were measured by DU72 UV–Vis spectrometer to test the absorption of HRP and Th. Amperometric responses of the TNT arrays (working electrode, the area was 0.5 cm^2) to H_2O_2 were investi-

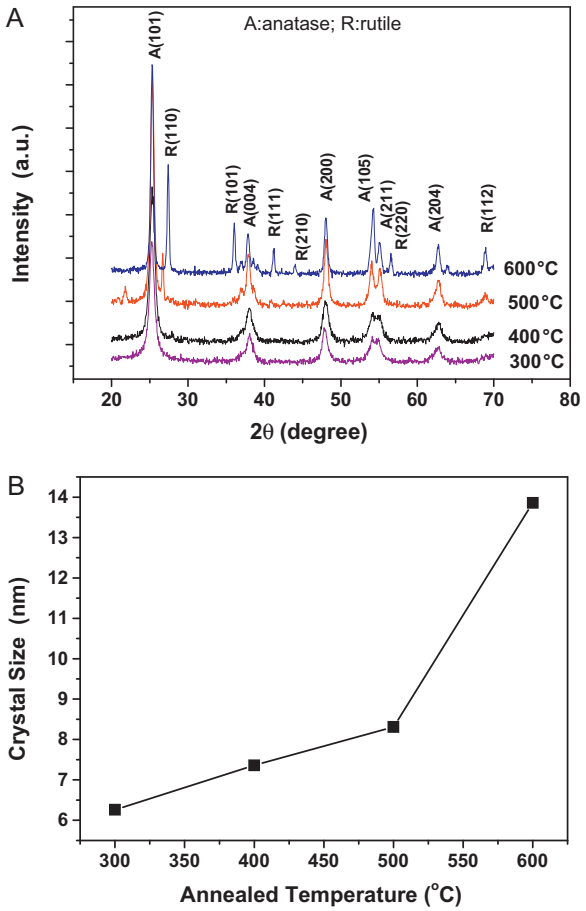

Fig. 2. (A) XRD patterns and (B) grain size of TNT arrays after annealed in CO for 3 h at 300 °C, 400 °C, 500 °C and 600 °C.

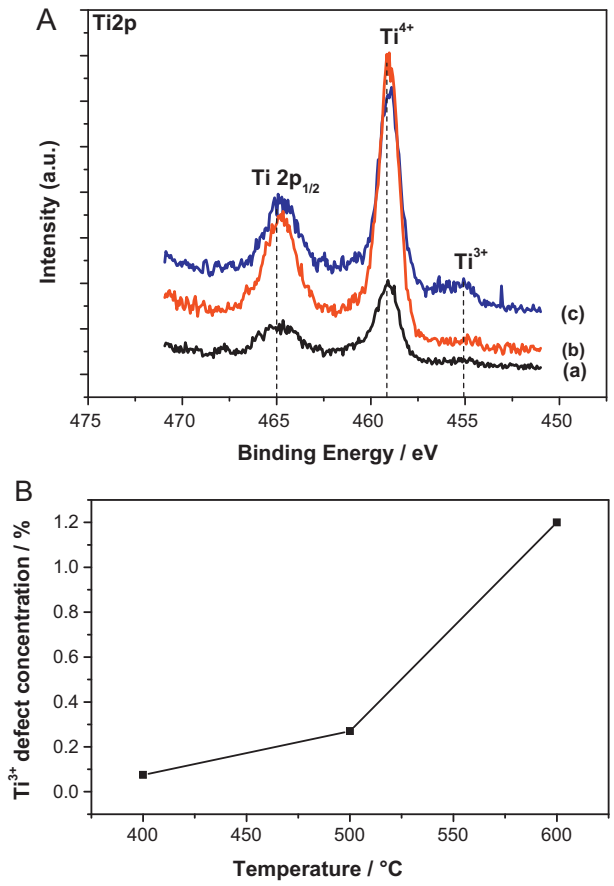

Fig. 3. (A)Ti2p XPS spectra of TNT arrays annealed in CO for 3 h at (a) 400 °C (b) 500 °C (c) 600 °C. (B) Ti^{3+} defect concentration as a function of annealing temperatures.

gated by an electrochemical workstation (CHI-6051C), where Pt foil and Ag/AgCl electrode were used as the counter electrode and the reference electrode respectively.

3. Results and discussion

3.1. Structural characterization of TNT arrays

Several different TNT arrays were investigated in our previous work on its biosensitivity towards H_2O_2. It was found that the nanotube formed by anodization in 0.1 M KF electrolyte showed biosensitivity that surpassed comparable nanotubes anodized in 0.1 M HF electrolyte [2]. Therefore, in the present work the same type of TNT arrays were used to investigate the surface defects doping on the sensitivity of TNT biosensor.

Fig. 1 shows the SEM images of TNT arrays before annealing (A), after annealing in CO at (B) 300 °C, (C) 400 °C, (D) 500 °C and (E) 600 °C for 3 h. The average diameter and wall thickness of TNT arrays were estimated from the SEM images and averaged over a large area. The as-grown TNT had an inner diameter of 92 nm, wall thickness of 8 nm and length of 1.5 μm. The length of the nanotubes decreased to 1.46 μm after annealing at 300 °C, while the inner diameter has no obviously change. After annealing at 400 °C, 500 °C, and 600 °C for 3 h, the inner diameter of TNT decreased to 88 nm, 85 nm, and 80 nm, the wall thickness increased to 12 nm, 15 nm, and 20 nm and the length of the nanotubes decreased to 1.42 μm, 1.3 μm and 1.1 μm, respectively. As expected, the increase of wall thickness was accompanied with a decrease in the length of TNT according to SEM cross-section images, such a morphology change was thermodynamically favorable during annealing treatment, where the reduction of specific surface area and thus the total surface energy were expected [17], resulting in the increase of wall thickness as well as the decrease in length of TNT. As a comparison, TNT morphology annealed in O_2 was more stable and could only be destroyed at temperature higher than 600 °C, which was in good agreement with what reported in literature [17]. In addition, annealing at 700 °C in CO for 3 h resulted in complete collapse of nanotube array structure and no nanotubes could be found after annealing at 700 °C or above.

Fig. 2 compares the XRD patterns of TNT arrays annealed in CO for 3 h at different temperatures. The anatase phase was the main crystalline phase in both samples annealed at 300 °C and 400 °C, however, the rutile phase was clearly detected in TNT arrays when the annealing temperature was higher than 500 °C. By analyzing the XRD peaks, the (1 0 1) peak of anatase phase was used to estimate the particle size of each TNT by the Scherer equation. It was found that the particle size correlated with the annealing temperature, the crystallite size of TNT/300 was estimated to be 6.26 nm, while the grain size of TNT/600 increased to 13.86 nm with the increase of annealing temperature. The relatively easy phase transition from anatase to rutile at 500 °C in CO gas compared to O_2 gas and the increase of grain size could possibly be ascribed to easier nucleation at the surface promoted by the surface defects that result from annealing in CO, which will be discussed further in the following section.

3.2. The formation of Ti^{3+} defects on TNT arrays

To understand the influence of Ti^{3+} defects in TNT arrays and also to quantify the amount of surface defects, Ti2p XPS spectra

Table 1
Peak current and potential separation of TNT arrays annealed in CO at different temperatures.

	300 °C	400 °C	500 °C	600 °C
i_{po} ($\times 10^{-4}$ A)	4.73	4.99	3.34	2.39
i_{pr} ($\times 10^{-4}$ A)	−4.31	−4.40	−2.84	−2.42
ΔE_p (V)	0.17	0.14	0.13	0.10

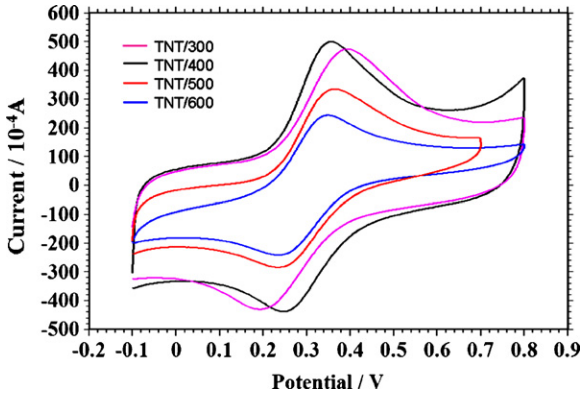

Fig. 4. CV curves of TNT array annealed in CO at different temperatures. The measurement were taken in 1 M KCl solution at 0.1 V/s in the presence of 10 mM $K_3[Fe(CN)_6]$.

(Fig. 3A) were recorded for TNT arrays annealed at 400 °C, 500 °C and 600 °C respectively where oxygen vacancies were supposed to be created by CO treatment.

Fig. 3(A) shows the Ti2p spectra of TNT annealed in CO at various temperatures. The peaks at binding energy of 465 eV and 458.8–454.9 eV were ascribed to $Ti2p_{1/2}$ and $Ti2p_{3/2}$ [18]. The peaks at 458.8, 456.8 and 454.9 eV were related to Ti^{4+}, Ti^{3+} and TiC species, respectively [19–21], indicating the existence of Ti^{3+} defects in TNT annealed in CO. It was also noticed that there was an energy shift for Ti^{3+} (2.0 eV) and TiC (3.9 eV) as manifested in Fig. 3(A). These intermediate oxidation states of titanium were formed by the reduction of TiO_2 during CO annealing as suggested in the literatures [12,22]. The Ti^{3+} defects concentration as a function of annealing temperatures is shown in Fig. 3(B), it was found that Ti^{3+} defects concentration was 0.075% for TNT/400, while increased to 0.27% for TNT/500 and 1.2% for TNT/600 with the increasing of annealing temperature.

3.3. Electrochemical properties of TNT arrays

Electrochemical properties of TNT arrays which had different surface defects concentrations were investigated by means of cyclic voltammetry (CV) with 10 mM $K_3[Fe(CN)_6]$ as an electrolyte in a potential range of −0.1 V to 0.8 V versus Ag/AgCl at a sweep rate of 0.1 V/s. Fig. 4 shows the CV curves of the four samples. A pair of well-defined oxidation/reduction peaks was observed for the four samples during the scanning process. The peak separation and peak currents were summarized in Table 1. As shown in Table 1, the peak currents of the samples decreased with the increase of annealing temperatures, this current decrease could be attributed

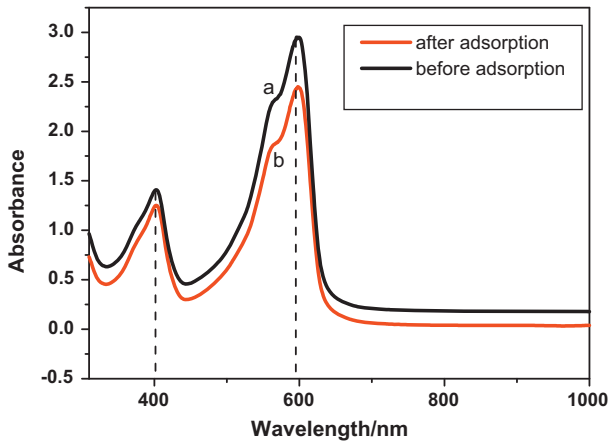

Fig. 5. UV–Vis absorbance spectra of (a) as-prepared mixture solution (1.8 mg Th and 3.6 mg HRP in 3 ml of 5 mM PB) and (b) the solution after absorbed by TNT arrays annealed in CO at 500 °C for 24 h.

to the reducing of surface area when the annealing temperature increased. At elevated temperatures, phase transformation or crystallization of TiO_2 will take place through nucleation, grain growth and densification process. Surface defects doped in the nanotubes after annealing in CO could rapid the grain growth of anatase phase to rutile phase, make the nanotube shrinkage or partially collapsed from the SEM side view as shown in Fig. 1(D) and (E). The shrinkage reduced the surface area of TNT and resulted in a lower current density. However, the peak separation decreased when the annealing temperature increased according to Table 1. The peak separations were 0.17 V for TNT/300 and enhanced to 0.10 V for TNT/600. The smaller the peak separation, the faster the electron transfer rate was. In our previous study, the average apparent heterogeneous electron transfer rate constant (k) was calculated to be 1.34×10^{-3} cm/s for TNT/500 according to its peak separation [15]. The enhanced electron transfer rate of TNT array annealing in CO could be attributed to the increase of trivalent titanium cations according to the XPS spectra.

3.4. Adsorption of HRP and Th on TNT arrays

Fig. 5 compares the UV–Vis absorption spectra of (a) as-prepared enzyme (HRP) and thionine chloride (Th) mixture solution and (b) the solution after absorbed by TNT/500 for 24 h. Both characteristic absorption peaks of HRP at 403 nm and Th at 599 nm were appreciably reduced, indicating partial HRP and Th were removed from the solution and adsorbed/immobilized onto the TNT electrode. The amounts of HRP and Th adsorbed were estimated from the 403 nm and 599 nm peak intensities, respectively. Table 2 summarized and compared the amounts of HRP and Th adsorbed onto the different TNT electrodes. These results revealed that the amount of HRP and Th adsorbed on TNT were affected by the Ti^{3+} defects concentration.

The amounts of HRP adsorbed onto the four samples were estimated to be 5.03 μg/cm², 6.72 μg/cm², 9.16 μg/cm² and 4.05 μg/cm², respectively. TNT/500 electrode demonstrated the

Table 2
Structure data and the absorbance of HRP and Th on different TNT arrays.

	Inner diameter (nm)	Wall thickness (nm)	Length (μm)	Surface area (cm²/cm²)	HRP adsorption (μg/cm²)	Th adsorption (μg/cm²)
As-grown TNT	92	8	1.50	42.2	3.23	11.78
TNT/300	90	10	1.46	41.3	5.03	13.85
TNT/400	88	12	1.42	38.7	6.72	16.43
TNT/500	85	15	1.30	34.7	9.16	17.58
TNT/600	80	20	1.10	20.6	4.05	10.18

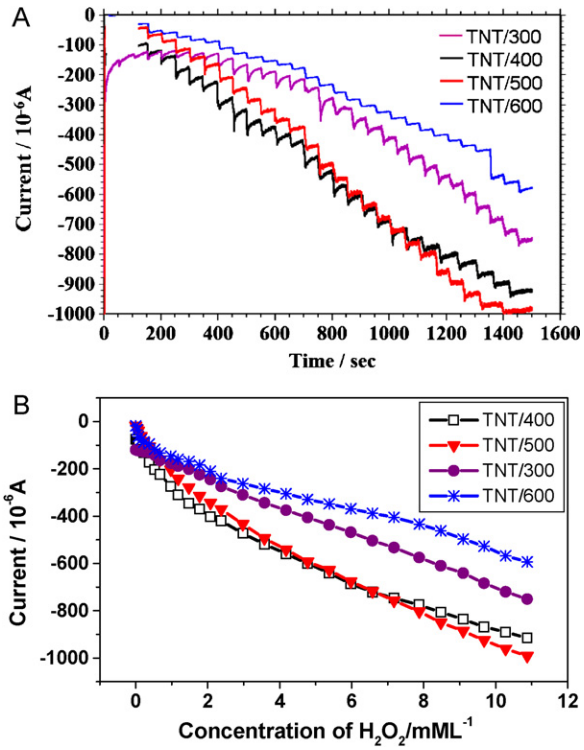

Fig. 6. (A) Amperometric response and (B) calibration plot of TNT biosensors to successive additions of 50 mM H_2O_2 solution.

highest adsorption density of HRP. According to our previous study [2], the amount of HRP adsorbed on TiO_2 nanotube surface played a determining role in the sensitivity of TNT electrode. It is possible that the presence of surface defects favors the adsorption of HRP molecules. The adsorption density of HRP on the as-grown TNT electrode was only 3.25 μg/cm^2, because almost no Ti^{3+} surface defect formed on this electrode. With the increase of annealing temperature, Ti^{3+} defect concentration increased, leading to the distinct improvement of HRP adsorption density for TNT/400 and TNT/500 electrodes. However, when the annealing temperature was above 600 °C, the specific surface area of TNT decreased due to the collapse and destruction of the nanotubes, resulting in the reduced amount of HRP adsorption for TNT/600 electrode.

3.5. Response of TNT biosensor to hydrogen peroxide

Fig. 6 shows the typical amperometric responses and calibration plots of the TNT biosensors to H_2O_2. The stable amperometric response was observed at −0.36 V with successive additions of 50 mM H_2O_2 into 0.1 M PB solution at pH 7.0. TNT/500 electrode displayed the largest amperometric response comparing with the other three samples. Its sub-linear response ranged from 1×10^{-5} M to 11.2×10^{-3} M and the polynomial fitting results of the curve was $C = -122.45 - 129.2I + 5.46I^2$, $R^2 = 0.991$ where C was the concentration of H_2O_2, I referred to the reduction current and R^2 was the correlation coefficients, the sensitivity for TNT/500 was 88.5 μA/mM l^{-1}, much improved than that of TNT/300 (58.2 μA/mM l^{-1}) and TNT/600 (46.7 μA/mM l^{-1}).

The poor biosensing performance of TNT/600 electrode is easy to understand, as TNT structure largely collapsed after annealing at 600 °C, thus the absorbance of HRP decreased, resulting in lower amperometric response. TNT/300 biosensor was also less sensitive than TNT/500, which could be ascribed to the relatively lower Ti^{3+} defects concentration. Ti^{3+} defects have been identified as being responsible for creation of hydroxyl groups on TNT surface due to dissociative adsorption of water. These hydroxyl groups could interact strongly with the reactive groups of the proteins polar amino acids. Hence reduced TNT surfaces would favor protein immobilization and improve titania biosensing properties. As indicated above, the concentration of Ti^{3+} defects in TNT/300 was lower than that in TNT/500, leading to less amount of HRP adsorbed onto the electrode. This result provided the evidence to support the idea that Ti^{3+} defects concentrations play a key role in the adsorption of protein or enzyme and the performance of TNT biosensors.

Furthermore, it was assumed that the sensing of hydrogen peroxide was through interface redox reactions mediated by both HRP and Th. Surface area and electrical properties of TNT arrays would affect the sensing limitation and sensitivity. Thus the response of TNT/500 should be more sensitive due to the better adsorption behavior of HRP and the faster electron transfer rate constant. Comparing with our former research [2], where the response range was from 1×10^{-5} M to 3×10^{-3} M for TNT electrode without annealing, the TNT biosensor annealed in CO exhibited wider response range and higher current response. In addition, this TNT biosensor annealed in CO retained 60% of its initial current response after storing for two weeks in 0.1 M PB solution at 4 °C, showing an acceptable shelf life.

4. Conclusions

In this study, we systematically investigated the influence of Ti^{3+} surface defects concentration on enzyme adsorption amount, electron transfer property as well as biosensitivity of TNT arrays fabricated by anodization. In order to doping TNT with different concentrations of Ti^{3+} defects, we used a thermally treatment in CO atmosphere at different temperatures. Successful Ti^{3+} defects doping was confirmed by XPS measurements. We have shown that annealing in CO at elevated temperatures ranging from 400 °C to 600 °C resulted in the increase of Ti^{3+} defects concentration in TNT arrays, which could enhance the electron transfer rate and the adsorption amount of enzyme for TNT. But the reduction of surface area would occur when the annealing temperature was higher than 600 °C due to the collapse of the nanotube. Thus, annealing in CO at 500 °C appeared to be the most favorable condition to achieve desirable nanotube array structure and surface defects density (0.27%), thus the TNT arrays presented the largest adsorption amount of HRP (9.16 μg/cm^2), faster electron transfer rate (1.34×10^{-3} cm/s) and the best response sensitivity (88.5 μA/mM l^{-1}).

Acknowledgements

Peng Xiao gratefully acknowledges the supporting of Science Foundation of Chongqing Science and Technology Committee (CSTS, 2009BB4047), the Fundamental Research Funds for the Central Universities (CDJXS10221142) and Sharing Fund of Chongqing University's large-scale equipment. This work is supported in part by National Science Foundation (DMI-0455994) and Air Force Office of Scientific Research (AFOSR-MURI, FA9550-06-1-032).

References

[1] X. Pang, D. He, S. Luo, Q. Cai, An amperometric glucose biosensor fabricated with Pt nanoparticle-decorated carbon nanotubes/TiO_2 nanotube arrays composite, Sens. Actuators B 137 (2009) 134–138.
[2] P. Xiao, B.B. Garcia, Q. Guo, D.W. Liu, G.Z. Cao, TiO_2 nanotube arrays fabricated by anodization in different electrolytes for biosensing, Electrochem. Commun. 9 (2007) 2441–2447.
[3] C. Guo, F. Hu, C.M. Li, P.K. Shen, Direct electrochemistry of hemoglobin on carbonized titania nanotubes and its application in a sensitive reagentless hydrogen peroxide biosensor, Biosens. Bioelectron. 24 (2008) 819–824.
[4] K.C. Popat, L. Leoni, C.A. Grimes, T.A. Desai, Influence of engineered titania nanotubular surfaces on bone cells, Biomaterials 28 (2007) 3188–3197.

[5] K.S. Brammer, S. Oh, J.O. Gallagher, S. Jin, Enhanced cellular mobility guided by TiO_2 nanotube surfaces, Nano Lett. 8 (2008) 786–793.
[6] J. Park, S. Bauer, K. Mark, P. Schmuki, Nanosize and vitality: TiO_2 nanotube diameter directs cell fate, Nano Lett. 7 (2007) 1686–1691.
[7] H. Tsuchiya, J.M. Macak, L. Müller, J. Kunze, F. Müller, P. Greil, S. Virtanen, P. Schmuki, Hydroxyapatite growth on anodic TiO_2 nanotubes, J. Biomed. Mater. Res. A 77A (2006) 534–541.
[8] J. Park, S. Bauer, P. Schmuki, K. Mark, Narrow window in nanoscale dependent activation of endothelial cell growth and differentiation on TiO_2 nanotube surfaces, Nano Lett. 9 (2009) 3157–3164.
[9] S. Oh, C. Daraio, L.H. Chen, T.R. Pisanic, R.R. Finones, S. Jin, Significantly accelerated osteoblast cell growth on aligned TiO_2 nanotubes, J. Biomed. Mater. Res. A 78A (2006) 97–103.
[10] K. Cai, M. Frant, J. Bossert, G. Hildebrand, K. Liefeith, K.D. Jandt, Surface functionalized titanium thin films: zeta-potential, protein adsorption and cell proliferation, Colloids Surf. B 50 (2006) 1–8.
[11] F. Guillemot, M.C. Porté, C. Labrugère, Ch. Baquey, Ti^{4+} to Ti^{3+} conversion of TiO_2 uppermost layer by low-temperature vacuum annealing: interest for titanium biomedical applications, J. Colloid Interface Sci. 255 (2002) 75–78.
[12] L.Q. Wang, D.R. Baer, M.H. Engelhard, Creation of variable concentrations of defects on TiO_2(1 1 0) using low-density electron beams, Surf. Sci. 320 (1994) 295–306.
[13] R. Wang, K. Hashimoto, A. Fujishima, M. Chikuni, E. Kojima, A. Kitamura, M. Shimohigoshi, T. Watanabe, Photogeneration of highly amphiphilic TiO_2 surfaces, Adv. Mater. 10 (1998) 135–138.
[14] R. Wang, K. Hashimoto, A. Fujishima, M. Chikuni, E. Kojima, A. Kitamura, M. Shimohigoshi, T. Watanabe, Light-induced amphiphilic surfaces, Nature 388 (1997) 431.
[15] P. Xiao, H. Fang, G. Cao, Y. Zhang, X. Zhang, Effect of Ti^{n+} defects on electrochemical properties of highly-ordered titania nanotube arrays, Thin Solid Films 518 (2010) 7152–7155.
[16] Y. Zhang, P. Xiao, X. Zhou, D. Liu, B.B. Garcia, G. Cao, Carbon monoxide annealed TiO_2 nanotube array electrodes for efficient biosensor applications, J. Mater. Chem. 19 (2009) 948–953.
[17] O.K. Varghese, D. Gong, M. Paulose, C.A. Grimes, E.C. Dickey, Crystallization and high-temperature structural stability of titanium oxide nanotube arrays, J. Mater. Res. 18 (2003) 156–165.
[18] W. Gopel, J.A. Anderson, D. Frankel, M. Jaehnig, K. Phillips, J.A. Schafer, G. Rocker, Surface defects of TiO_2(1 1 0): a combined XPS, XAES AND ELS study, Surf. Sci. 139 (1984) 333–346.
[19] J.M. Macak, H. Tsuchiya, P. Schmuki, High-aspect-ratio TiO_2 nanotubes by anodization of titanium, Angew. Chem. Int. Ed. Engl. 44 (2005) 2100–2102.
[20] L.I. Johansson, Electronic and structural properties of transition-metal carbide and nitride surfaces, Surf. Sci. Rep. 21 (1995) 177–250.
[21] J. Zhao, E.G. Garza, K. Lam, C.M. Jones, Comparison study of physical vapor-deposited and chemical vapor-deposited titanium nitride thin films using X-ray photoelectron spectroscopy, Appl. Surf. Sci. 158 (2000) 246–251.
[22] D. Leinen, A. Fernandez, J.P. Espinos, A.R. Gonzalez-Elipe, Chemical effects in TiO_2 and titanates due to bombardment with Ar^+ and O_2^+ ions of different energies (3.5–10 keV), Appl. Phys. A 63 (1996) 237–242.

Biographies

Dr. Peng Xiao received her Ph.D. at the Chongqing University, China, in the area of condense matter physics in 2008. She is an associate professor of the Physics College in Chongqing University. Her interests include synthesis of metal oxide nanomaterials and matrixes for biosensor/immuno sensor applications.

Dr. Yunhuai Zhang received his Ph.D. in materials science in 2004 at the Chongqing University, China. He is a professor of the College of Chemical Engineering at the Chongqing University. His interests include nanomaterials synthesis by chemical method and its application on catalysis and photoelectrocatalysis.

Prof. Guozhong Cao held a Ph.D. on ceramics materials from Eindhoven University of Technology, Netherlands in 1991. He is a professor in Department of Materials Science & Engineering at the University of Washington and takes a particular interest in synthesis nanomaterials, electrochemical batteries, supercapacitors and nanostructured oxides for solar cells.